0026-895X/97/040725-10$3.00/0

MOLECULAR PHARMACOLOGY, **52:**725–734 (1997).

Effects of Protein Phosphatase and Kinase Inhibitors on Ca^{2+} and Cl^- Currents in Guinea Pig Ventricular Myocytes

YOSHIYUKI HIRAYAMA and H. CRISS HARTZELL

Department of Anatomy and Cell Biology, Emory University School of Medicine, Atlanta, Georgia 30322-3030

Received April 8, 1997; Accepted June 18, 1997

SUMMARY

It is well-established that in heart, both the L-type Ca^{2+} channel and the cystic fibrosis transmembrane conductance regulator Cl^- channel are regulated by cAMP-dependent phosphorylation. However, it is not clear whether both of these channels are regulated in concert by protein kinase A (PKA) or whether there are mechanisms that independently control the phosphorylation of these two PKA targets. The purpose of this study was to compare the effects of various protein phosphatase and protein kinase inhibitors on these two ionic currents (I_{Ca} and I_{Cl}) in guinea pig ventricular myocytes to gain insight into these questions. We found that both the stimulation and washout of the effects of isoproterenol on I_{Cl} are about twice as fast as the effects on I_{Ca}, probably because the dephosphorylation reaction for I_{Cl} is faster than that for I_{Ca}. In contrast, inhibition of protein phosphatases with 10 μM microcystin stimulated both I_{Ca} and I_{Cl}, but the stimulation of I_{Cl} was much slower and smaller than the stimulation of I_{Ca}. The effect of microcystin was inhibited by staurosporine (K_i = 171.5 and 161 nM for I_{Ca} and I_{Cl}, respectively), suggesting that the stimulation was due to a kinase. The kinase was not protein kinase C (PKC) because it was not inhibited by the specific pseudosubstrate inhibitor of PKC, $PKC_{(19-31)}$, and it was not PKA because it was not inhibited by adenosine 3′,5′-cyclic phosphorothioate. These results suggest that although both the Ca^{2+} and Cl^- channels are regulated by cAMP-dependent phosphorylation, another protein kinase may also regulate these channels, and the kinetics of the response of the channels to phosphorylation can be modulated independently by protein phosphatases.

In mammalian cardiac myocytes, β-adrenergic agonists regulate a variety of ionic currents, including I_{Ca} and I_{Cl} (1–3). Both currents are stimulated by cAMP-dependent phosphorylation via the G_s/adenylyl cyclase/cAMP/PKA cascade, but both of these currents may be regulated by phosphorylation of more than a single phosphorylation site.

In the case of I_{Ca}, Tsien *et al.* (4) proposed that two different phosphorylation sites were responsible for the β-adrenergic regulation of Ca^{2+} channel availability (N) and channel gating (P_o). Support for this hypothesis has come from studies on rabbit ventricular myocytes in which different concentrations of okadaic acid selectively affect N and p_o (5) and from our studies on frog ventricular myocytes in which the amplitude of I_{Ca} is regulated by two phosphorylation sites that can be distinguished by the phosphatases that dephosphorylate them (6). One site is dephosphorylated by phosphatase 2A, and the other site is dephosphorylated by a phosphatase with a low sensitivity to the phosphatase inhibitors microcystin, okadaic acid, and calyculin A.

The regulation of I_{Cl} is even more complicated (3). The regulation of this channel, like that of the Ca^{2+} channel, involves two phosphorylation sites. One site is dephosphorylated by protein phosphatase 2A, and the other is dephosphorylated by a phosphatase with a low sensitivity to microcystin and okadaic acid, which may be protein phosphatase 2C (7). In addition, the channel is regulated by ATP binding and hydrolysis by its two nucleotide binding domains. The singly phosphorylated channel exhibits brief openings that correspond to hydrolysis of ATP by the first nucleotide binding site. The doubly phosphorylated channel exhibits a much longer channel open time that involves ATP binding to the second nucleotide binding site and stabilization of channel open state.

Although it is clear that both channels are regulated by PKA, there is evidence that other protein kinases may also be involved in their regulation as well. For example, PKC can regulate cardiac Ca^{2+} channels (8), and the CFTR Cl^- channel may also be regulated by PKC (3). Furthermore, we have recently shown that in frog ventricular myocytes there is a novel protein kinase, which we have termed PKX, that can

This work was supported by National Institutes of Health Grant HL21195.

ABBREVIATIONS: PKA, protein kinase A; CFTR, cystic fibrosis transmembrane conductance regulator; E_{Cl}, Cl^- equilibrium potential; E_{rev}, reversal potential; Fsk, forskolin; I_{Ca}, L-type Ca^{2plus} current; I_{Cl}, cAMP-activated Cl^- current; Iso, isoproterenol; myr-$PKC_{(19-31)}$, myristoylated derivative of the pseudosubstrate protein kinase C inhibitor; PKC, protein kinase C; PKX, protein kinase X; TPA, 12-*O*-tetradecanoylphorbol-13-acetate; EGTA, ethylene glycol bis(β-aminoethyl ether)-*N*,*N*,*N*′,*N*′-tetraacetic acid; HEPES, 4-(2-hydroxyethyl)-1-piperazineethanesulfonic acid; R_p-cAMPS, adenosine 3′-5′-cyclic phosphorothioate.

phosphorylate one of the phosphorylation sites that regulates I_{Ca} (6).

The fact that both I_{Ca} and I_{Cl} seem to be regulated by two phosphorylation sites and that multiple protein kinases can regulate these channels raises the question of whether these channels are regulated in concert or independently by phosphorylation. For example, when cAMP levels increase in the cell, do both channels become phosphorylated with the same kinetics, or can the phosphorylation of each channel be adjusted independently? One way that phosphorylation could be adjusted would be by alterations in the activity of the protein phosphatases responsible for dephosphorylation. For these reasons, we decided to compare the regulation of I_{Ca} and I_{Cl} by β-adrenergic agonists and inhibitors of protein phosphatases and kinases in guinea pig ventricular myocytes.

Materials and Methods

Isolation of cardiac myocytes. Single guinea pig ventricular myocytes were isolated by enzymatic dissociation. Female guinea pigs, weighing 300–400 g, were anesthetized with sodium pentobarbital (50 mg/kg). The chest was opened under artificial respiration, and the aorta was cannulated for perfusion with Tyrode's solution before the heart was removed from the animal. After the perfusate was changed to nominally Ca^{2+}-free Tyrode's solution for ~5 min, a nominally Ca^{2+}-free Tyrode's solution with 0.1–0.11 mg/ml collagenase (Yakult Co., Tokyo, Japan) was recirculated for ~9 min using a Langendorff apparatus. After the enzyme was washed out, the hearts were then stored in high-K^+ and low-Cl^- solution at room temperature (22°) for 10 min. The isolated cells were obtained by gentle agitation of small pieces of ventricle and stored in the high-K^+ and low-Cl^- solution for 1 hr. They were then kept in Tyrode's solution at room temperature before use.

Solutions. The composition of the Tyrode's solution was 144 mM NaCl, 0.33 mM NaH_2PO_4, 4.0 mM KCl, 1.8 mM $CaCl_2$, 0.53 mM $MgCl_2$, 5.5 mM glucose, and 5.0 mM HEPES-NaOH buffer, pH adjusted to 7.4 with NaOH. Nominally Ca^{2+}-free Tyrode's solution simply omitted $CaCl_2$. High-K^+ and low-Cl^- solution contained 70 mM glutamic acid, 15 mM taurine, 30 mM KCl, 10 mM KH_2PO_4, 0.5 mM $MgCl_2$, 11 mM glucose, 0.5 mM EGTA, and 5.0 mM HEPES-NaOH buffer, pH adjusted to 7.4 with KOH. The internal solution for recording I_{Ca} contained 85 mM CsCl, 10 mM EGTA, 20 mM tetraethylammonium Cl, 10 mM MgATP, 2 mM $MgCl_2$, 5 mM pyruvic acid, 5 mM $Tris_2$-creatine phosphate, 0.1 mM Tris-GTP, 5.5 mM glucose, and 10 mM PIPES, pH to 7.15 with CsOH. External solution contained 130 mM NaCl, 20 mM CsCl, 1.8 mM $CaCl_2$, 0.5 mM $MgCl_2$, 5.5 mM glucose, and 5 mM HEPES, pH to 7.3 with CsOH. In some experiments, 0.02 mM ouabain was added to suppress Na-K pump currents (9). In Fig. 5, the composition of the 158 mM Cl^- external solution was the same as the standard external solution except that 2 mM $CoCl_2$ replaced the 1.8 mM $CaCl_2$. The 28.6 mM Cl^- solution was the same as the 158 mM Cl^- solution except that NaCl was replaced with Na-aspartate. The bath was continuously superfused with control solution at a rate of ~2 ml/min, and the patch-clamped cell could be exposed to different test solutions within 1 sec by placing the cell at the mouth of one of a group of capillary tubes attached to reservoirs flowing at ~100 μl/min.

The internal solution was changed as previously described (6). Briefly, a fine polyethylene tube was inserted to within 250 μm of the tip of the patch pipette. At the onset of the experiment, the other end of the tubing was placed in a reservoir containing control internal solution while the gigaohm seal was being made and broken. Measurements of control currents were made while control solution was being perfused into the pipette. Then, the negative pressure was released, and the tubing was switched to another reservoir containing the experimental drug dissolved in the control solution. The new solution was then aspirated into the patch pipette by again applying negative pressure to the patch pipette holder.

Drugs. Reagents included cAMP-dependent protein kinase inhibitor peptide R_p-cAMPS (gift of Dr. Ira Cohen, State University of New York, Stony Brook, NY); microcystin-LR (GIBCO BRL, Gaithersburg, MD); K252a, staurosporine, and Fsk (Calbiochem, San Diego, CA); calyculin A (LC Laboratories, Woburn, MA); TPA (Sigma Chemical, St. Louis, MO); and myr-$PKC_{(19–31)}$ (Promega, Madison, WI). Stock solutions of staurosporine were prepared at 1 mM in dimethylsulfoxide. Microcystin was made at a concentration of 0.5 mM in 10% methanol. Fsk was 10 mM in 100% ethanol. Stock solutions were stored at −20°.

Recording methods. Whole-cell currents were recorded using a patch-clamp amplifier (EPC-7; List Medical Instruments, Darmstadt, Germany). Cells were patch-clamped with borosilicate patch pipettes with a resistance of 1–2 MΩ. Total series resistance was usually <3 MΩ. I_{Ca} was elicited by voltage pulses delivered by a programmable digital stimulator (Challenger DB; W. Goolsby, Kinetic software and Emory University, Atlanta, GA). Routine pulses were from −50 to 0 mV. The pulse was 200 msec in duration, and I_{Ca} was measured as the peak inward current minus the current at the end of the pulse. Because the reversal potential of I_{Cl} (E_{Cl}) was measured to be −7 mV and calculated to be −10 mV and because I_{Cl} at −50 mV was small relative to I_{Ca}, contamination of I_{Ca} by I_{Cl} at 0 mV should be negligible. I_{Cl} was measured as the steady state current at −50 mV. Experiments were conducted at room temperature unless otherwise stated.

Results

Kinetics of stimulation of I_{Ca} and I_{Cl} by Iso. Initially, we were interested in comparing the time course of the effects of β-adrenergic stimulation on I_{Ca} and I_{Cl} in guinea pig ventricular myocytes to gain insights into possible differences in the regulation of these two currents (Fig. 1). Myocytes were voltage-clamped using the whole-cell configuration of the patch-clamp technique. K^+ currents were blocked by internal tetraethylammonium and internal and external cesium. The inward Na^+ current was blocked by holding the membrane potential at −50 mV. Myocytes were routinely depolarized from a holding potential of −50 to 0 mV for 200 msec at a frequency of 0.1 sec^{-1}. The depolarization elicited a transient inward current that was completely blocked by Ca^{2+} channel blockers. I_{Ca} was measured as the difference between the peak inward current and the current at the end of the depolarizing pulse. I_{Cl} was measured as the steady state current at −50 mV. The current at −50 mV that is stimulated by Iso is I_{Cl} under these conditions because the reversal potential (E_{rev}) of this current obtained by voltage ramps was near E_{Cl} (data not shown). Because I_{Ca} was measured near the E_{rev} for I_{Cl}, there was little contamination of I_{Ca} by I_{Cl}.

In Fig. 1A, 1 μM Iso increased I_{Ca} 3.5-fold and increased I_{Cl} to 2.2 pA/pF. I_{Ca} was stimulated more slowly than I_{Cl}. Fig. 1B shows the time course of change of the normalized currents. The time to half-maximum stimulation was 12.0 sec for I_{Cl} and 24.6 sec for I_{Ca} (Fig. 1B). On washing out Iso, I_{Ca} also decreased more slowly than I_{Cl}. The time to half-maximum deactivation was 1.6 min for I_{Cl} and 3.1 min for I_{Ca}. On average, the half-times of activation and inactivation for I_{Ca} were 25.8 ± 0.6 sec and 3.6 ± 0.2 min, respectively (five cells), and the half-times of activation and inactivation for I_{Cl} were 12.0 ± 0.2 sec and 2.1 ± 0.2 min, respectively (six cells). In Fig. 1B, it seems that I_{Cl} in this cell may have washed out

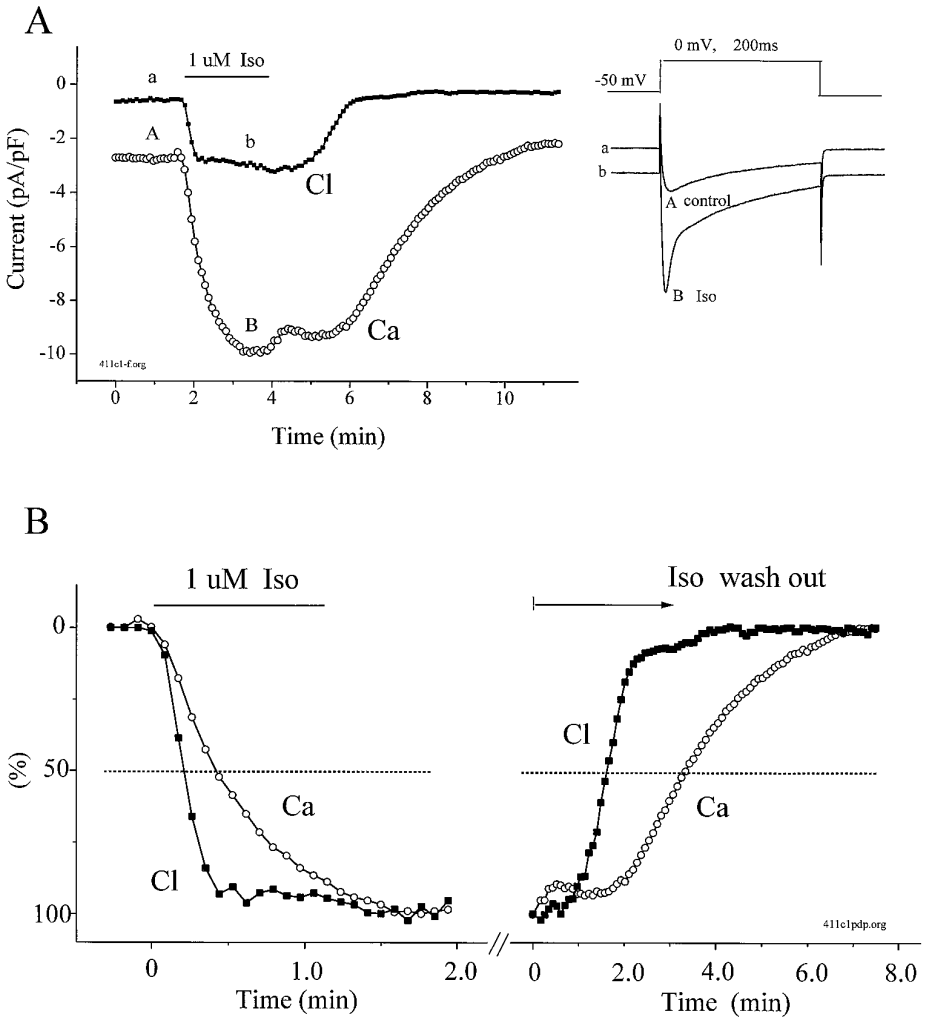

Fig. 1. Effect of Iso on I_{Ca} (○) and I_{Cl} (■) in guinea pig ventricular myocytes. A, Time course of the effect of Iso; 1 μM was added to the superfusion (*bar*). Representative current traces are shown for control (A, *a*) and after Iso (B, *b*). B, Comparison of onset and washout of the effect of Iso on I_{Ca} and I_{Cl}. Currents were normalized to the maximum current stimulated by Iso.

with two kinetic components, one fast and one slow. This was not a routine observation.

Effects of protein phosphatase inhibitors on I_{Ca} and I_{Cl}. To investigate further the phosphorylation reactions controlling these currents, we examined the effects of protein phosphatase inhibitors. Fig. 2A shows the effects of internal perfusion of the myocyte with the protein phosphatase inhibitor microcystin. The bar indicates the period when microcystin was added to the internal solution. On changing the internal solution, there was a ~3-min lag period before I_{Ca} increased. This was partly due to the dead volume of the internal perfusion system. I_{Ca} increased from 2.2 to 11.0 pA/pF in 13 min in response to 10 μM microcystin. However, I_{Cl} did not begin to increase until after I_{Ca} had nearly reached its maximum (11 min after changing the internal solution); then, I_{Cl} increased very slowly. At 18 min after the addition of 10 μM microcystin, I_{Cl} was 1.2 pA/pF. Microcystin (10 μM) stimulated both I_{Ca} and I_{Cl}, but I_{Ca} always increased more rapidly than I_{Cl}. The subsequent application of Fsk stimulated I_{Cl} markedly but had little effect on I_{Ca}.

Fig. 2, B and C, shows the effects of lower concentrations of microcystin. These lower concentrations of microcystin (1 or 3 μM) had no effect on I_{Cl} and had only minimal effects on basal I_{Ca}. However, subsequent application of 10 μM Fsk produced a large, rapid increase in both currents. Both currents remained partially elevated after Fsk washout. Thus, lower concentrations of microcystin seemed to inhibit a phosphatase responsible for dephosphorylation of sites phosphorylated by PKA but did not significantly stimulate the currents in the absence of PKA activity.

The very slow stimulation of I_{Cl} by microcystin shown in Fig. 2A was in contrast to the rapid stimulation of I_{Cl} relative to I_{Ca} by Iso in Fig. 1. The relative difference in the kinetics of stimulation of I_{Ca} and I_{Cl} by Iso and microcystin suggests that there are interesting differences in how phosphorylation regulates these channels.

Fig. 3 shows the dose-response curves for the effect of microcystin alone on I_{Ca} (Fig. 3A) and I_{Cl} (Fig. 3B). The effects of microcystin on both I_{Ca} and I_{Cl} were measured ~2–5 min after the effect of microcystin on I_{Ca} had plateaued. Because the effect of microcystin on I_{Cl} is much slower than the effect on I_{Ca}, the dose-response curve for I_{Cl} was not obtained in a steady state condition and may actually underestimate the steady state effect of microcystin. However, it was not practical to wait until the effect on I_{Cl} reached a plateau. Despite this limitation, the data demonstrate that the effect of microcystin was quantitatively less on I_{Cl} than it was on I_{Ca} over the same time period. Both currents were activated by microcystin at a threshold concentration of ~3 μM . Data were fitted to the Hill equation (lines). The best-fit parameters were I_{Ca}, $K_{½}$ = 4.6 μM, I_{max} = 5.5 pA/pF; and I_{Cl}, $K_{½}$ = 7.0 μM, I_{max} = 1.46 pA/pF. The

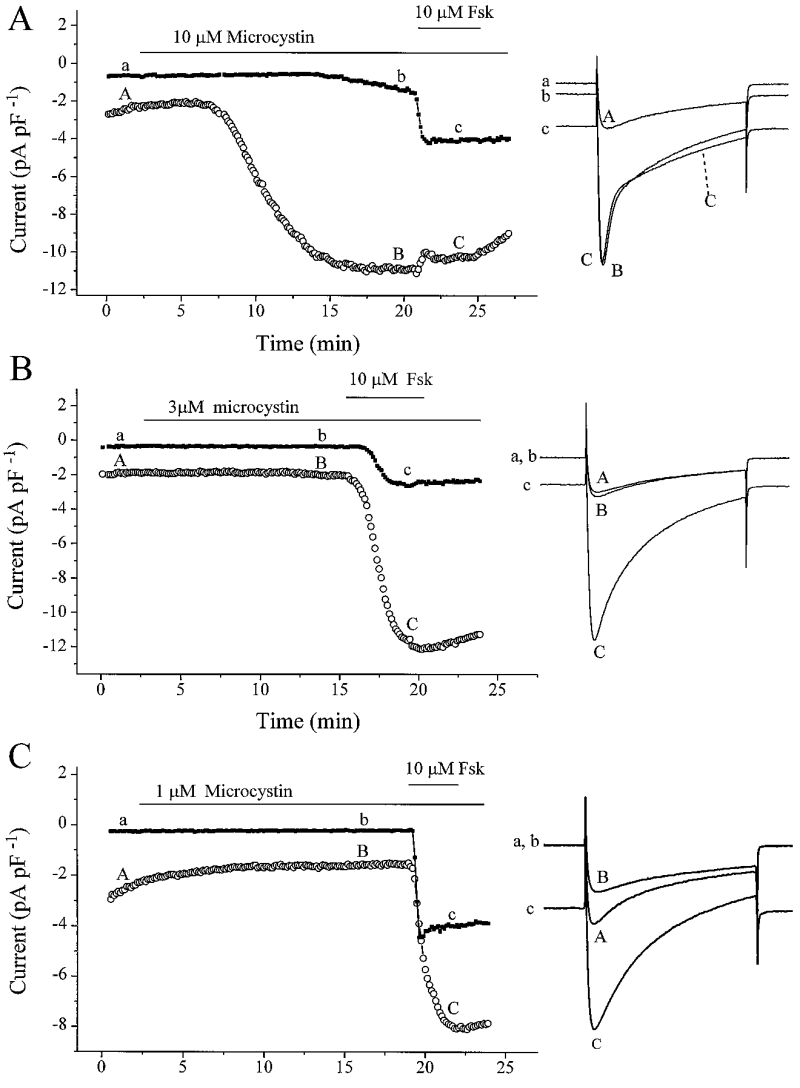

Fig. 2. Effects of the protein phosphatase inhibitor microcystin on I_{Ca} and I_{Cl}. A, 10 μM microcystin was applied by internal perfusion, and 10 μM Fsk was applied to the superfusion as indicated. Internal perfusion was begun at the time indicated, but ~3 min was required for the new solution to reach the tip of the pipette. Microcystin increased both I_{Ca} (○) and I_{Cl} (■), but I_{Cl} increased more slowly than I_{Ca}. B, 3 μM microcystin increased I_{Ca} a small amount but had no effect on I_{Cl} (*trace B*). The subsequent application of 10 μM Fsk produced a large and rapid increase in both currents (*trace C*). C, Effect of internal perfusion with 1 μm microcystin. Neither I_{Ca} nor I_{Cl} was stimulated by microcystin alone.

effects of microcystin on I_{Ca} and I_{Cl} are compared in Fig. 3C. At 20 μM, microcystin alone was able to stimulate I_{Ca} as much as microcystin plus Iso, but in the same time period, the same concentration of microcystin alone was able to stimulate I_{Cl} only ~40% compared with the stimulation of I_{Cl} produced by microcystin plus Iso. This suggests that whatever kinases are responsible for the increases in I_{Ca} produced by microcystin alone are not as effective in stimulating I_{Cl}.

The I_{Ca} stimulated by microcystin had the same biophysical properties as the basal I_{Ca}. Fig. 4A shows that the shape of the peak current-voltage relationship of I_{Ca} was unaffected by microcystin, but the current was increased in amplitude at all potentials. The activation curve and inactivation curve also were not affected (Fig. 4, B and C).

The microcystin-stimulated current at −50 mV is carried by Cl^-. For work described in the preceding paragraphs, we assumed that the current at −50 mV stimulated by high concentrations of microcystin (Fig. 2A) was I_{Cl}. To verify this, we measured the current-voltage relationship of the microcystin-induced current. The current-voltage relationship was determined by voltage ramps from −50 to +50 mV at 0.34 V/sec (Fig. 5). In these experiments, we used the standard external solution except that 2 mM $CoCl_2$ replaced 1.8 mM $CaCl_2$ to eliminate I_{Ca}. Fig. 5A shows current-voltage relations before and after internal perfusion with 10 μM microcystin. The microcystin-stimulated current was obtained by subtracting the before-perfusion value from the after-perfusion value (Fig. 5B). The current-voltage relationship was essentially linear with a small amount of outward rectification. The current reversed at −7.3 mV, which was very close to E_{Cl} (−9.6 mV). To verify that the current was a Cl^- current, we changed the bath $[Cl^-]_o$. The mean current-voltage relations of the microcystin-induced current with 28.6 and 158 mM $[Cl^-]_o$ were determined as the difference between the average of five records obtained in the absence and presence of microcystin (Fig. 5C). The reversal potential was −7.1 ± 1.9 mV with 158 mM $[Cl^-]_o$ and shifted to +36.2 ± 3.9 mV with 28.6 mM $[Cl^-]_o$. These values were almost identical to the calculated E_{Cl} value in each condition (E_{Cl} = −9.6 and +34.8 mV in 158 and 28.6 mM $[Cl^-]_o$, respectively, with $[Cl^-]_i$ = 109 mM). The dotted lines indicate the current-voltage relationship calculated from the Goldmann-Hodgkin-Katz equation (10) assuming a simple Cl^- conductance. From these data, we conclude that the microcystin-stimulated background current was carried by Cl^-. Because intracellular Ca^{2+} is highly buffered, it is unlikely this is a Ca^{2+}-activated Cl^- conductance and thus it is probably the CFTR Cl^- channel.

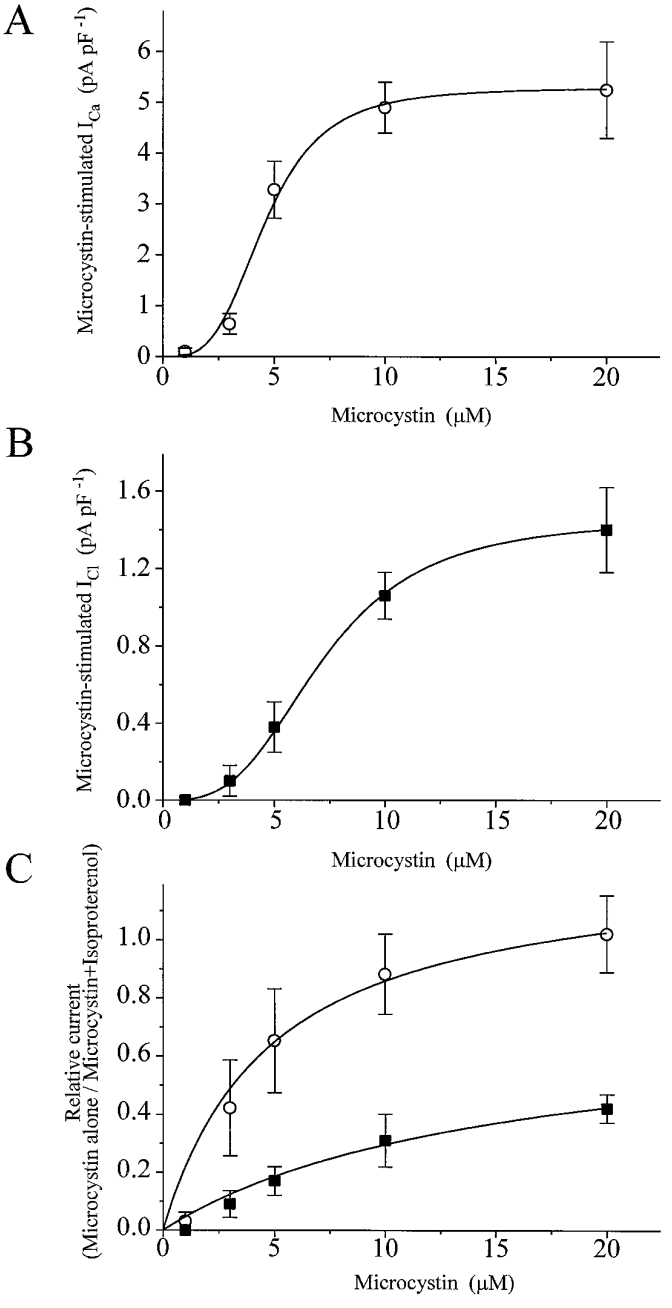

Fig. 3. Dose-response curve for the effect of microcystin on I_{Ca} (A) and I_{Cl} (B). Data points represent mean (5–13 cells) increase in I_{Ca} and I_{Cl} produced by a single internal application of microcystin. Data were fitted to the Hill equation (*lines*). The best-fit parameters were I_{Ca}, $K_{½}$ = 4.6 μM, I_{max} = 5.5 pA/pF; and I_{Cl}, $K_{½}$ = 7.0 μM, I_{max} = 1.46 pA/pF. C, Microcystin-stimulated current relative to current stimulated in the presence of microcystin and Fsk together. ○, I_{Ca}. ■, I_{Cl}. The best-fit parameters were I_{Ca}, $K_{½}$ = 4.8 μM, I_{max} = 1.27 pA/pF; and I_{Cl}, $K_{½}$ =15.0 μM, I_{max} = 0.74 pA/pF.

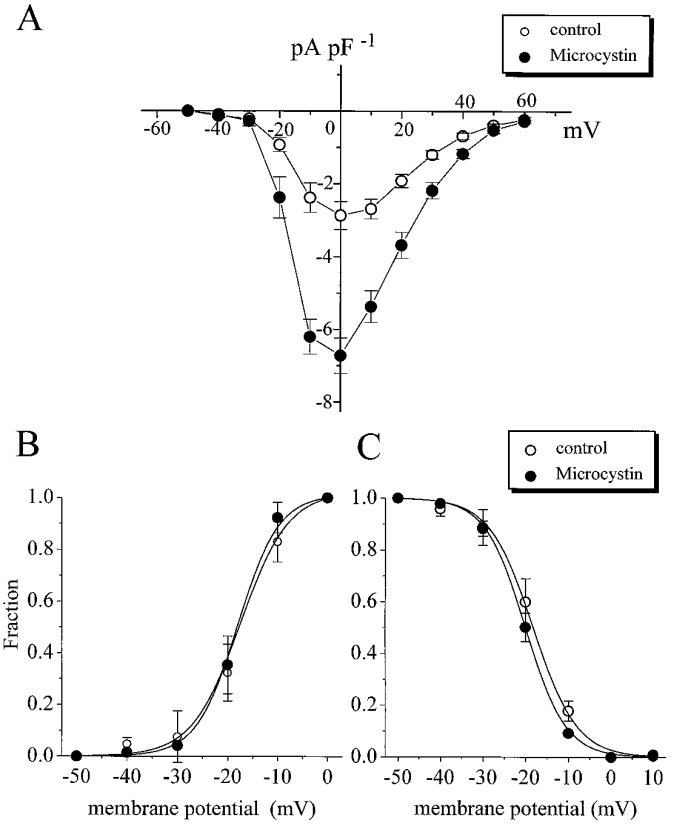

Fig. 4. Effects of microcystin on current-voltage relationship, activation, and inactivation curves of I_{Ca}. A, Peak current-voltage relationships before (○) and after (●) addition of 10 μM microcystin. Values are mean of five cells. B, Activation curves. The values were normalized to the maximum I_{Ca}. *Continuous curves*, fits to the Boltzmann relation. The half-maximal activation voltage (½) was −17.5 mV for control and −18.0 mV after the addition of 10 μM microcystin. C, Inactivation curve obtained by a double-pulse protocol before (circo]) and after (●) addition of 10 μM microcystin. The double-pulse protocol consisted of a 200-msec test pulse to 0 mV preceded by various conditioning prepulses of 2-sec duration between −50 and +10 mV separated by a 3-msec repolarization to −80 mV. Values for V½ were −18.2 mV for control and −20.0 mV after addition of 10 μM microcystin.

Effects of microcystin at 36°. The results in Fig. 2 differ somewhat from those of Hwang *et al.* (7), who showed that after washout of Fsk in the presence of microcystin, I_{Cl} decreased to a level ~25% of the maximally stimulated current. In contrast, we found that the effect of Fsk on I_{Cl} in the presence of 10 μM microcystin was nearly irreversible (Fig. 2A). One difference between our experiments and their experiments was that ours were performed at room temperature, whereas theirs were performed at 36°. When we repeated our experiments at 36° (Fig. 6, A and B), the stimulatory effects of 10 μM microcystin on I_{Ca} and I_{Cl} were qualitatively the same as at room temperature. Subsequent exposure to Fsk caused an rapid increase in I_{Cl}, but in contrast to the results at room temperature, washout of Fsk was followed by a ~75% decrease in I_{Cl} (Fig. 6, A and B). These results confirm those of Hwang *et al.* (7) and suggest that the difference between our result and theirs is due to higher phosphatase activity at 36°, which results in a partial dephosphorylation of I_{Cl}.

Inhibitory effects of microcystin and Fsk on I_{Ca}. The experiments at 36° revealed a very interesting aspect of I_{Ca} regulation that was less evident but also present at room temperature. Although I_{Ca} was stimulated by internal perfusion with 10 μM microcystin at 36°, subsequent exposure to Fsk produced a complex response in I_{Ca}. Initially, I_{Ca} rose quickly, but after ~30 sec, it began to decline. This decline continued even after Fsk was washed out. These results suggested that at 36°, Fsk may have triggered an event that caused a decrease in Ca^{2+} channel activity. Additional evi-

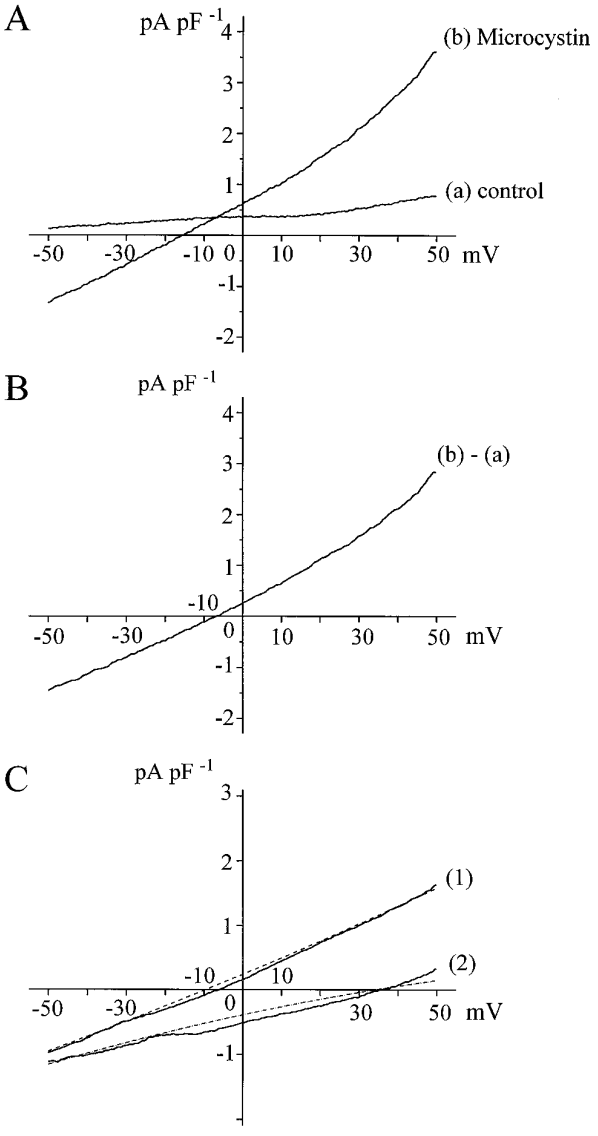

Fig. 5. Current-voltage relationship of the microcystin-stimulated background current. A, Current-voltage relationships obtained by triangular ramp pulses (−50 to +50 mV, dV/dt = 0.34 V/sec) before (a) and after (b) application of 10 μM microcystin. B, Current-voltage relationship of the microcystin-stimulated background current obtained after subtracting *a* from *b* in A. C, Effect of changing external $[Cl^-]_o$ on current-voltage relations for the microcystin-stimulated background current. 1, 158 mM $[Cl^-]_o$. 2, 28.6 mM $[Cl^-]_o$. $[Cl^-]_i$ was 109 mM. E_{rev} at 158 mM $[Cl^-]_o$ was −7.1 ± 1.9 mV. E_{rev} at 28.6 mM $[Cl^-]_o$ was +36.2 ± 3.9 mV. Values are mean of four or five cells. *Dotted lines*, current-voltage relation calculated from the Goldmann-Hodgkin-Katz equation assuming a pure Cl^- conductance.

dence for this inhibitory effect of Fsk can be seen at room temperature (Fig. 2A); I_{Ca} in the presence microcystin alone was stable for ~5 min, but after exposure to Fsk, I_{Ca} began to decrease, although I_{Cl} did not change.

To examine this effect in more detail, we examined the effect on I_{Ca} and I_{Cl} of another protein phosphatase inhibitor, calyculin A. Fig. 6C shows the effects of calyculin A and calyculin A plus Iso on I_{Ca}, and Fig. 6D shows the effects on I_{Cl}. Iso stimulated I_{Cl} to approximately the same degree, regardless of the concentration of calyculin A present. The amplitudes of the Cl^- currents in the presence of any concentration of calyculin and Iso were not significantly different than the amplitude in the absence of calyculin (>5%, *t* test). In contrast, the stimulation of I_{Ca} by Iso decreased as the calyculin A concentration increased over the same range. The amplitude ot the Ca^{2+} current in the presence of Iso and 150 nM calyculin was significantly different than the amplitude in the absence of calyculin (<1%, *t* test). These results suggest the possibility that there is an inhibitory phosphorylation that is potentiated by protein phosphatase inhibitors that selectively affects I_{Ca}. The fact that I_{Cl} is not affected shows that the effect is not a nonspecific effect.

Effects of protein kinase inhibitors on the response of I_{Ca} and I_{Cl} to microcystin. We hypothesize that microcystin stimulates I_{Ca} and I_{Cl} because there is a basally active protein kinase whose activity is counteracted by a basally active protein phosphatase. When the phosphatase is inhibited by microcystin, the phosphoprotein can accumulate and the current amplitude increases. In our studies on frog cardiomyocytes, we showed that the effect of microcystin required ATP and was blocked by protein kinase inhibitors (6, 11). To test whether the same mechanism could explain the effect of microcystin in guinea pig, we examined the ability of staurosporine to block the effects of microcystin (Fig. 7). Staurosporine, which is a nonspecific protein kinase inhibitor (12, 13), did block the effect of microcystin on I_{Ca} and I_{Cl}. Staurosporine was applied extracellularly at concentrations of 100–300 nM before internal perfusion with 20 μM microcystin was begun. At 300 nM, staurosporine decreased basal I_{Ca} and nearly completely inhibited the increase in I_{Ca} and I_{Cl} produced by microcystin (Fig. 7A). Even though 300 nM staurosporine nearly completely blocked the response of I_{Ca} and I_{Cl} to microcystin, subsequent application of Fsk produced large increases in both currents. Fig. 7B shows the dose-response curve for the effect of staurosporine on the microcystin-stimulated current. The EC_{50} values for inhibition of the effect of staurosporine on I_{Ca} and I_{Cl} were 171.5 and 161 nM, respectively. On average, in the presence of 300 nM staurosporine, microcystin-stimulated I_{Ca} and I_{Cl} were 0.48 ± 0.13 and 0.46 ± 0.22 pA/pF, respectively. In comparison, I_{Ca} and I_{Cl} values in the presence of 300 nM staurosporine, 20 μM microcystin, and 10 μM Fsk were 5.5 ± 0.79 and 3.4 ± 0.43 pA/pF, respectively. These results suggest that staurosporine inhibits a protein kinase that is responsible for stimulation of I_{Ca} and I_{Cl} by microcystin but that staurosporine at these concentrations has only a small effect on PKA.

Another interpretation that must be entertained is that staurosporine inhibits the action of microcystin nonspecifically via a mechanism independent of protein kinase inhibition. Although we cannot absolutely exclude this possibility, there are a number of reasons why this seems unlikely. First, in frog myocytes, in which microcystin produces a stimulation of I_{Ca} and an inhibition of the delayed rectifier K^+ current I_K, only the stimulation of I_{Ca} is inhibited by staurosporine (6). Therefore, the action of staurosporine is not nonspecific. Second, it seems clear that a kinase is involved in the action of microcystin on I_{Ca} because the effect requires ATP and is blocked not only by staurosporine but also by other kinase inhibitors such as K252a and H7 (6). Furthermore, the inhibitory effect of staurosporine is only observed if it is applied before the stimulatory effect of microcystin has occurred. If staurosporine is applied after microcystin has already stimulated the current, staurosporine is unable to inhibit the current. This behavior is consistent with a mech-

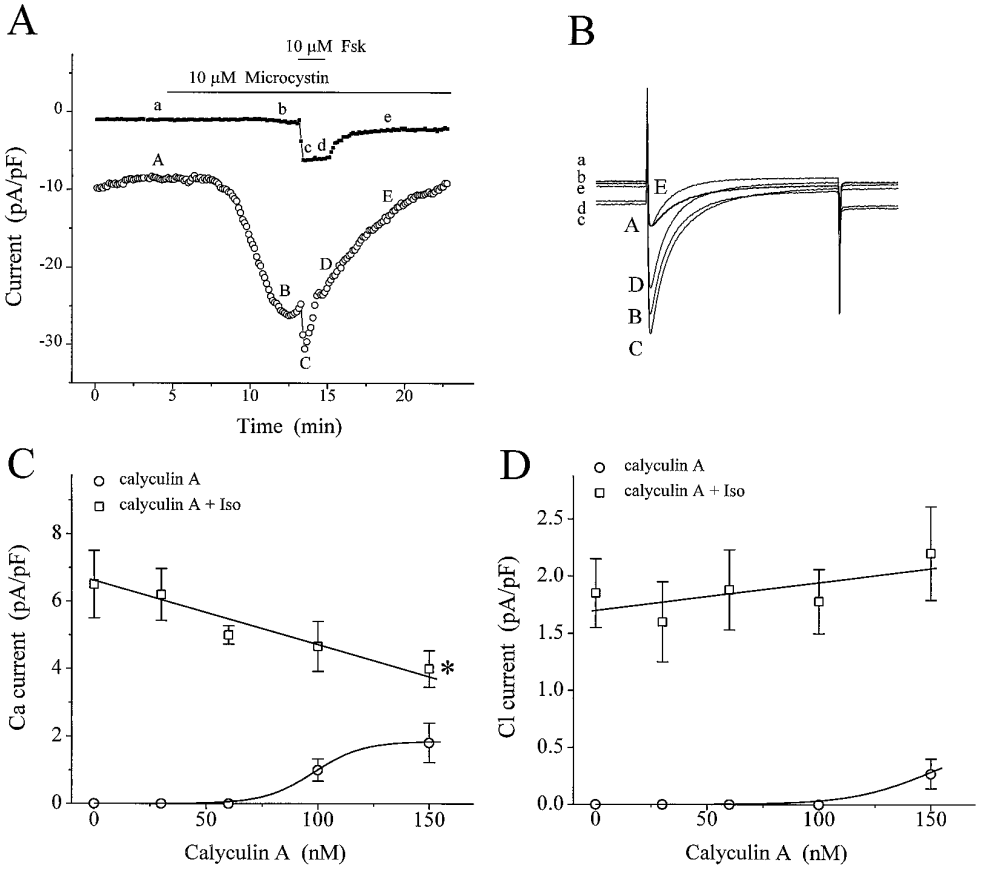

Fig. 6. Inhibitory effects of microcystin and Fsk on I_{Ca} and I_{Cl} at 36° and room temperature. At 10 μM, microcystin was perfused internally, and 10 μM Fsk was added to the superfusion as indicated. A, Temperature = 36°. The amplitudes of I_{Ca} (○) and I_{Cl} (■) are plotted versus time. B, Sample traces from the experiment shown in A. C, Temperature = 22°. Dose-response curve for the effect of calyculin A on I_{Ca}. ○, I_{Ca} density stimulated by calyculin A alone. □, I_{Ca} density in the presence of calyculin and Iso. D, Dose-response curve for the effect of calyculin A on I_{Cl}. ○, I_{Cl} density stimulated by calyculin A alone. □, I_{Cl} density in the presence of calyculin and Iso. Values in C and D are mean of 4–10 cells. *, Statistical significance from current in the absence of calyculin at 1% level (*t* test).

anism involving microcystin inhibiting a phosphatase and staurosporine inhibiting a kinase because one would expect staurosporine to have no effect once phosphorylation had taken place in the presence of an inhibitor of dephosphorylation (microcystin). It is difficult to propose a nonspecific mechanism of staurosporine action that has this behavior. Because a kinase is clearly involved in the response to microcystin and because the effect of microcystin is blocked by staurosporine, a known kinase inhibitor, we favor the simplest interpretation that staurosporine blocks the effect of microcystin by inhibition of a kinase.

Staurosporine also reduced basal I_{Ca}. On average, 300 nM staurosporine reduced basal I_{Ca} by 29.5 ± 10.1% (six cells). This decrease did not seem to be rundown because the effect of staurosporine was rapid. This suggests that the basal amplitude of I_{Ca} may be determined by a kinase that is basally active and inhibited by staurosporine.

PKA inhibition has no effect on the response of I_{Ca} and I_{Cl} to microcystin. To determine which protein kinases might be responsible for the stimulation of these currents by microcystin, we examined the effects of the competitive PKA inhibitor R_p-cAMPS on the responses of I_{Ca} and I_{Cl} to 10 μM microcystin (Fig. 8A). In this experiment, the cells were first perfused internally with 2 mM R_p-cAMPS, which had very little effect on basal I_{Ca}. After ~7-min internal perfusion with R_p-cAMPS, neither I_{Ca} nor I_{Cl} responded to 1 μM Iso, showing that PKA had been inhibited. However, the subsequent addition of 10 μM microcystin to the internal perfusion produced a large stimulation of both I_{Ca} and I_{Cl}. To be certain that PKA had been completely inhibited, we also performed this experiment in a different order (Fig. 8B). In this cell, R_p-cAMPS completely blocked PKA because Fsk had no effect on either I_{Ca} or I_{Cl} when added after microcystin perfusion, but microcystin was still capable of increasing both currents. The mean values for 10 μM microcystin-stimulated I_{Ca} and I_{Cl} in the presence of R_p-cAMPS were 6.0 ± 0.4 and 1.1 ± 0.1 pA/pF, respectively (six cells). The mean values for 10 μM microcystin-stimulated I_{Ca} and I_{Cl} without R_p-cAMPS were 4.9 ± 0.5 and 1.0 ± 0.12 pA/pF, respectively (15 cells). These results show that the effects of microcystin on I_{Ca} or I_{Cl} were not mediated by phosphorylation catalyzed by PKA.

PKC inhibition has no effect on the response of I_{Ca} and I_{Cl} to microcystin. Staurosporine is a nonselective protein kinase inhibitor, and it inhibits PKC *in vitro* at submicromolar concentrations (13). This suggests the possibility that the basally active protein kinase that stimulates I_{Ca} and I_{Cl} in the presence of microcystin is PKC. PKC is known to activate I_{Ca} in guinea pig ventricular myocytes (14), but it is controversial whether PKC regulates I_{Cl} (3). Fig. 9A shows the effect of the PKC activator TPA (0.1 μM) on I_{Ca} and I_{Cl}. I_{Ca} began to increase within 1 min after exposure to TPA and reached 11.3 pA/pF. I_{Cl} began to increase more slowly than I_{Ca} and reached a density of 2.3 pA/pF. Thus, it seems that both currents may be regulated by PKC. To determine whether the effect of microcystin could be explained by PKC-dependent phosphorylation, we examined the effects of a highly selective pseudosubstrate PKC inhibitor.

For these experiments, we used the myristoylated derivative of the peptide pseudosubstrate inhibitor $PKC_{(19–31)}$; the myristoylated derivative has been reported to be a more effective inhibitor of PKC because it is targeted to the membrane (15). In Fig. 9B, 100 μM myr-$PKC_{(19–31)}$ was applied

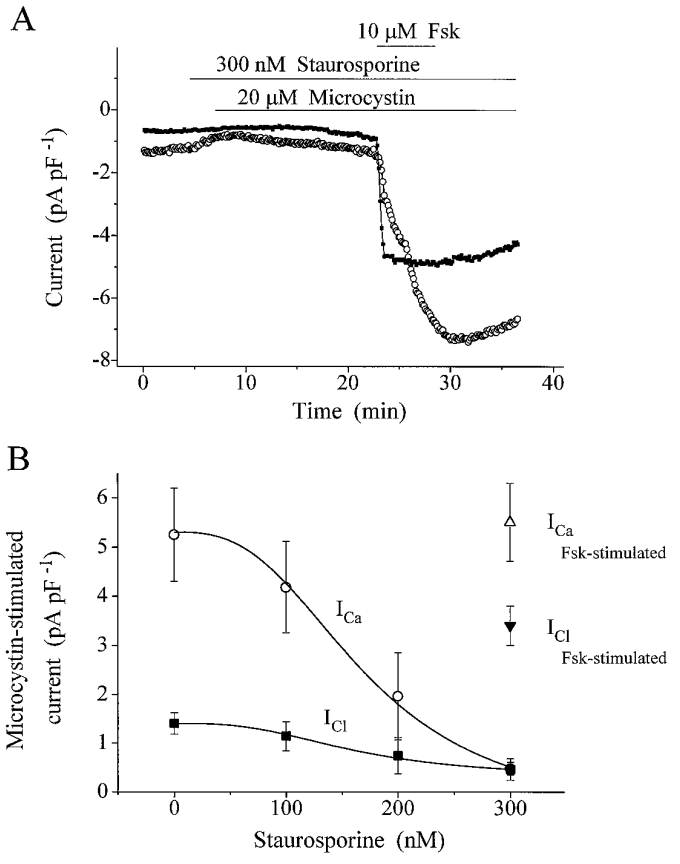

Fig. 7. Effect of the protein kinase inhibitor staurosporine on the response of I_{Ca} and I_{Cl} to microcystin. ○, I_{Ca}. ■, I_{Cl}. A, 300 nM staurosporine and 10 μM Fsk were applied by superfusion, and 20 μM microcystin was applied by internal perfusion during the times indicated. Staurosporine decreased basal I_{Ca} and inhibited the effect of microcystin on I_{Ca} and I_{Cl}. Subsequent application of Fsk produced a large increase in I_{Ca} and I_{Cl} even in the presence of staurosporine. B, Dose-response curve for the effect of staurosporine on microcystin-stimulated I_{Ca} and I_{Cl}. Data were fitted to the power logistic equation (*lines*). EC_{50} values were 171.5 nM for I_{Ca} and 161 nM for I_{Cl}. Response of I_{Ca} (△) and I_{Cl} (▼) to 10 μM Fsk in the presence of 300 nM staurosporine and 20 μM microcystin (five cells).

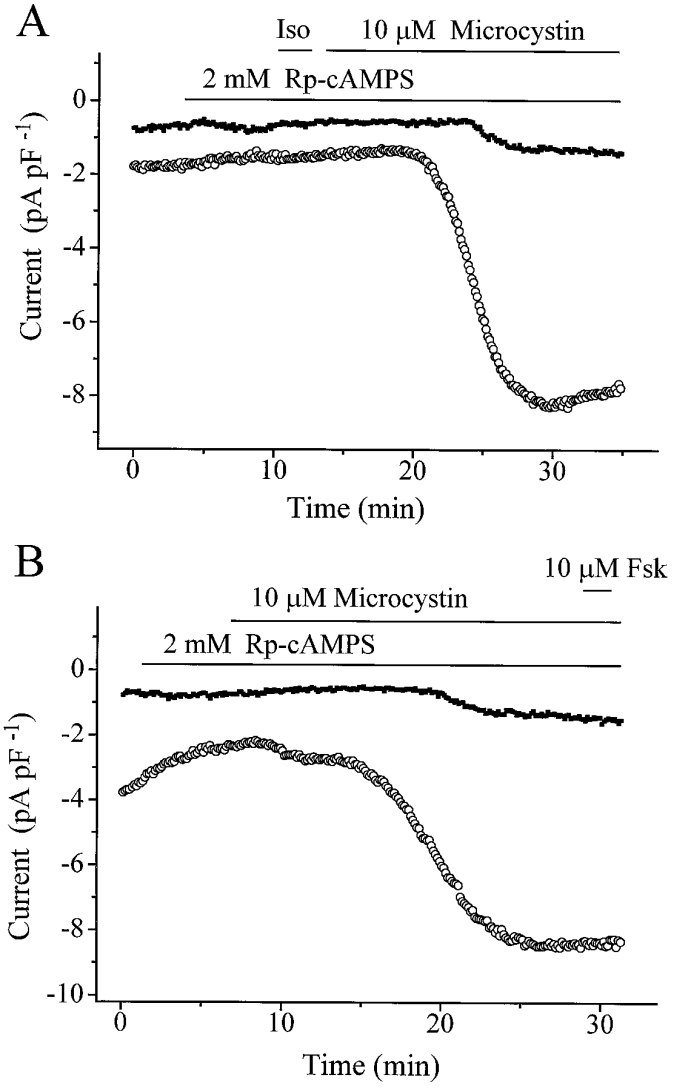

Fig. 8. Effect of the PKA inhibitor R_p-cAMPS on the response of I_{Ca} and I_{Cl} to 10 μM microcystin and 1 μM Iso (A) or 10 μM Fsk (B). ○, I_{Ca}. ■, I_{Cl}. Cells were first perfused internally with 2 mM R_p-cAMPS, which had no effect on basal I_{Ca}. A, Response to Iso and microcystin. B, Response to microcystin and Fsk.

internally with 2 mM R_p-cAMPS. After a 6-min perfusion with myr-$PKC_{(19–31)}$ and R_p-cAMPS, 0.1 μM TPA had no effect on I_{Ca} or I_{Cl}. However, 10 μM microcystin increased both I_{Ca} and I_{Cl} to 7.1 and 1.8 pA/pF, respectively. These results show that stimulation of I_{Ca} and I_{Cl} by microcystin is not mediated by PKC.

Discussion

I_{Ca} and I_{Cl} are regulated independently by phosphorylation. These data show that although both I_{Ca} and I_{Cl} are regulated by PKA phosphorylation, their regulation is not necessarily coordinate. For example, the increases in amplitude of I_{Ca} and I_{Cl} produced by Iso occur with different kinetics. I_{Cl} increases more rapidly than I_{Ca} in response to stimulation by Iso; the washout of the Iso effect is also faster. If we assume that the rate-limiting step regulating the amplitudes of I_{Ca} and I_{Cl} is a phosphorylation reaction, $D \rightleftarrows P$, then the rate of increase in the current will be proportional to $\alpha + \beta$ and deactivation will be proportional to β, where α is the forward rate constant and β is the backward rate constant. Because both the stimulation and washout of the Iso effect were faster for I_{Cl}, we conclude that the dephosphorylation reaction for I_{Cl} is faster than that for I_{Ca}. We do not currently have any insights into why dephosphorylation of I_{Cl} may be faster than I_{Ca}; possibilities include different phosphatase isoforms responsible for dephosphorylation of the two channels or differences in the rate of dephosphorylation of the different substrates by the same phosphatase.

I_{Ca} and I_{Cl} are regulated by PKA and another protein kinase. The observation that I_{Cl} was more rapidly dephosphorylated than I_{Ca} suggested that application of a protein phosphatase inhibitor might result in a larger basal stimulation of I_{Cl} than I_{Ca}. However, we found that I_{Cl} increased much less and more slowly than I_{Ca} in response to protein phosphatase inhibitors. This difference in the kinetics of response of the two currents to Iso and microcystin was explained by the fact that the increase in both basal currents produced by microcystin was not caused by PKA but by another, as yet unidentified, protein kinase. The fact that the

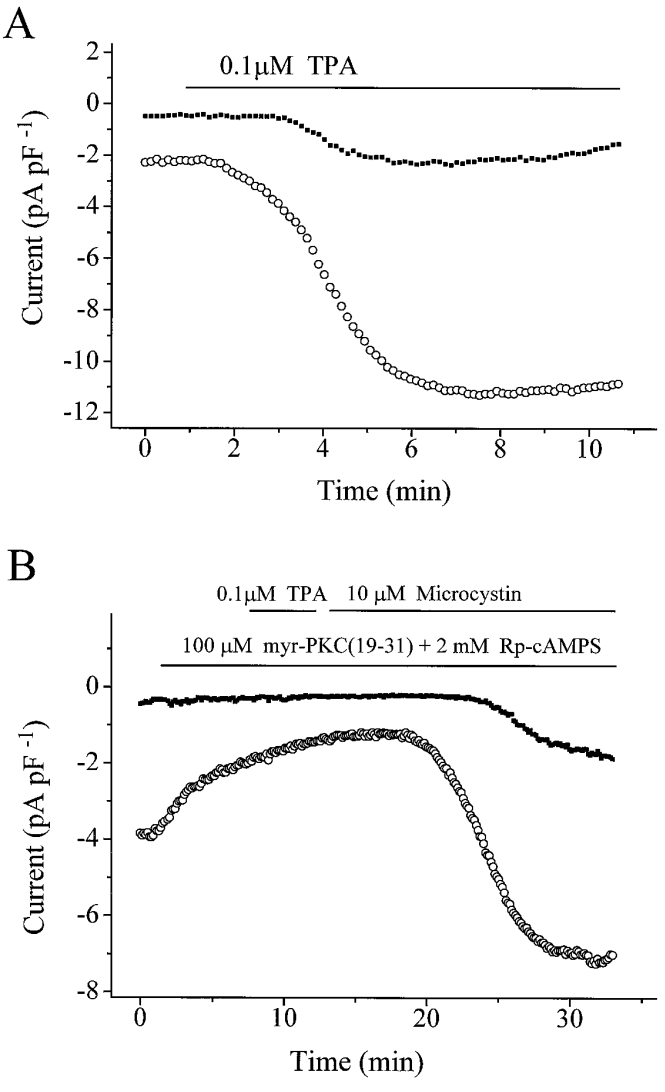

Fig. 9. Regulation of I_{Ca} and I_{Cl} by PKC and microcystin. ○, I_{Ca}. ■, I_{Cl}. A,. Effects of the PKC activator TPA on I_{Ca} and I_{Cl}. At 0.1 μM, TPA was applied to the bath solution during the time indicated (*bar*). I_{Ca} began to increase within 1 min after exposure of TPA. I_{Cl} began to increase slower than I_{Ca}. B, Effects of a PKC pseudosubstrate inhibitor on the response of I_{Ca} and I_{Cl} to microcystin; 100 μM myr-$PKC_{(19-31)}$ was applied internally with 2 mM R_p-cAMPS. After a 6-min perfusion with myr-$PKC_{(19-31)}$ and R_p-cAMPS, 0.1 μM TPA had no effect on basal I_{Ca} and I_{Cl}. Subsequent internal perfusion with 10 μM microcystin increased both I_{Ca} and I_{Cl} to 7.1 and 1.8 pA/pF, respectively.

effects of microcystin are blocked by low concentrations of the nonselective protein kinase inhibitor staurosporine, however, argues that the effect of microcystin is mediated through a phosphorylation reaction. This protein kinase is clearly not PKA because it is not inhibited by PKA inhibitors, which in the same cell do inhibit the effect of Iso or Fsk. Likewise, the kinase is not PKC because the peptide inhibitors of PKC that inhibit the effects of TPA in the same cell do not inhibit the effects of microcystin. Finally, it is unlikely that the kinase is a Ca^{2+}-dependent kinase because the cells were perfused internally with 10 mM EGTA, which should inhibit the activation of Ca^{2+}-dependent protein kinases. This novel protein kinase is very similar to one we described in frog ventricular myocytes and have termed PKX (6, 11).

We believe that the microcystin-stimulated current at −50 mV is the CFTR Cl^- current (16–18) for the following reasons. (1) The current at −50 mV that is stimulated by microcystin is a Cl^- current because it has a reversal potential near E_{Cl} and the reversal potential changes as predicted with changes in $[Cl^-]_o$. Furthermore, the current-voltage relationship is the same as reported for the cAMP-activated Cl^- current. (2) The current does not resemble other Cl^- currents that have been described in cardiac muscle, including a stretch-activated Cl^- current (19, 20), a Ca^{2+}-activated Cl^- current (21, 22), and a PKC-activated Cl^- current (23, 24). Collier and Hume (25) recently reported that this PKC-activated Cl^- current was the CFTR Cl^- current in guinea pig ventricular myocytes. It is unlikely that the current is a Ca^{2+}-activated Cl^- current because intracellular Ca^{2+} is highly buffered with EGTA. Furthermore, the fact the microcystin-stimulated current is time independent and requires phosphorylation to be activated suggests it is the CFTR Cl^- current.

Differences in the rates of phosphorylation/dephosphorylation by PKA and PKX could be due to differences in the association of kinases and phosphatases with Cl^- and Ca^{2+} channels. For example, PKX might be more closely associated with Ca^{2+} channels than Cl^- channels such that Ca^{2+} channels are phosphorylated preferentially. This possibility is made more attractive by recent studies that have identified several "scaffold" proteins that bind and target a variety of signaling enzymes to appropriate locations in the cell (26, 27). Recently, it was shown that voltage-dependent potentiation of L-type Ca^{2+} channels requires a cAMP-anchoring protein (28) and that L-type Ca^{2+} channels are associated with a 15-kDa cAMP-anchoring protein (29). Thus, differential regulation of different ion channels by protein kinases and phosphatases may be affected by differential localization of the kinases and phosphatases to the immediate neighborhood of the channel.

Physiological role of PKX. We hypothesize that the role of PKX in ventricular myocytes may be to regulate the basal level of I_{Ca}. Our reasons for suggesting this hypothesis are discussed below. The basal level of I_{Ca} is not determined by PKA-dependent phosphorylation because we find that internal perfusion of guinea pig myocytes with the PKA inhibitor R_p-cAMPS did not have a significant effect on basal I_{Ca} (see, for example, Fig. 8A). Ono and Fozzard (30) reported that the phosphatase inhibitor okadaic acid slowed rundown of Ca^{2+} channel activity in excised inside-out patches. They suggested that dephosphorylation was an important component of rundown and that phosphorylation was needed for channel-opening activity under basal conditions. They speculated that the intact cell may have protein kinases other than PKA that could maintain some level of phosphorylation. This is consistent with our results, and we conclude PKX may be important for maintaining basal phosphorylation of I_{Ca} in guinea pig ventricular myocytes. In support of this suggestion is the observation that 300 nM staurosporine reduced basal I_{Ca}, which may reflect basal activation of I_{Ca} by PKX.

Hescheler *et al.* (31, 32) have also reported that cell dialysis with protein phosphatase 1 inhibitor or okadaic acid stimulated basal I_{Ca} and suggested that there was a high activity of intracellular protein kinase even in the absence of agonist that was normally counteracted by a high level of protein phosphatase activity.

The role of PKX in regulating I_{Cl} is less clear. I_{Cl} is stim-

ulated much more slowly and to a much lesser extent than I_{Ca}. Thus, it is not clear that this phosphorylation is physiologically relevant. The observation that I_{Cl} is activated slowly by phosphatase inhibitors suggests that the Cl^- channel is also a substrate for PKX but that either the Cl^- channel is a relatively poor substrate for PKX or protein phosphatases that are insensitive to microcystin keep the accumulation of the phosphorylated state low. Cheng *et al.* (33) detected basal levels of phosphorylation in CFTR Cl^- channel and suggest that basal phosphorylation sites do not represent PKA sites in CFTR Cl^- channel. In contrast, Nakashima and Ono (34) observed that the phosphatase inhibitor okadaic acid increased I_{Cl}, but they speculated that this was due to basal activity of PKA.

Inhibitory effects of PKA stimulation in the presence of protein phosphatase inhibitors. Another novel finding of these studies is that Fsk or Iso in the presence of microcystin or calyculin A seemed to have a dual effect on I_{Ca}; initially, Fsk or Iso stimulated I_{Ca}, but then it initiated a run-down of I_{Ca}. This decrease in I_{Ca} was not paralleled by any change in I_{Cl}, suggesting that run-down of I_{Ca} was not due to deterioration of the cell or to activation of a nonselective microcystin-insensitive phosphatase. The effect was observed with both Fsk and Iso, suggesting that the effect was not due to a pharmacological effect of Fsk but rather to activation of the cAMP cascade. This run-down phenomenon was much more pronounced at 36°. The decrease in the amplitude was accompanied by increased inactivation of the current, supporting the idea that the effect was specific.

In conclusion, we found that I_{Ca} and I_{Cl} are stimulated by phosphatase inhibitors in the absence of β-adrenergic stimulation. The conclusion that this stimulatory effect is mediated by a basally active kinase is supported by the observation that this effect is inhibited by a protein kinase inhibitor. The kinase is not PKA nor PKC because it is not inhibited by PKA or PKC inhibitors. We speculate that this kinase, which we term PKX, contributes to set the basal level of I_{Ca} but plays a lesser role in regulation of the CFTR Cl^- channel.

Acknowledgments

We thank A. Rinderknecht and Drs. L. Quarmby, A. Ivanov, K. Machaca, S. Mierergerd, and K. Uchida for comments on the manuscript.

References

1. Hartzell, H. C. Regulation of cardiac ion channels by catecholamines, acetylcholine and second messenger systems. *Prog. Biophys. Mol. Biol.* **52:**165–247 (1985).
2. McDonald, T. F., S. Pelzer, W. Trautwein, and D. J. Pelzer. Regulation and modulation of calcium channels in cardiac, skeletal, and smooth muscle cells. *Physiol. Rev.* **74:**365–507 (1994).
3. Gadsby, D. C., G. Nagel, and T. C. Hwang. The CFTR chloride channel of mammalian heart. *Annu. Rev. Physiol.* **57:**387–416 (1995).
4. Tsien, R. W., B. P. Bean, P. Hess, J. B. Lansman, B. Nilius, and M. C. Nowycky. Mechanism of calcium channel modulation by β-adrenergic agents and dihydropyridine calcium agonists. *J. Mol. Cell Cardiol.* **18:**691–710 (1986).
5. Ono, K., and H. A. Fozzard. Two phosphatase sites on the Ca^{2+} channel affecting different kinetic functions. *J. Physiol. (Lond.)* **470:**73–84 (1993).
6. Hartzell, H. C., Y. Hirayama, and J. Petit-Jacques. Effects of protein phosphatase and kinase inhibitors on the cardiac L-type Ca current suggest two sites are phosphorylated by protein kinase A and another protein kinase. *J. Gen. Physiol.* **106:**393–414 (1995).
7. Hwang, T. C., M. Horie, and D. C. Gadsby. Functionally distinct phosphoforms underlie incremental activation of protein kinase-regulated Cl^- conductance in mammalian heart. *J. Gen. Physiol.* **101:**629–650 (1993).
8. Hartzell, H. C., and A. Rinderknecht. Calphostin C, a widely used protein kinase C inhibitor, directly and potently blocks L-type Ca channels. *Am. J. Physiol.* **270:**C1293–C1299 (1996).
9. Matsuoka, S., T. Ehara, and A. Noma. Chloride-sensitive nature of the adrenaline-induced current in guinea-pig cardiac myocytes. *J. Physiol.* **425:**579–598 (1990).
10. Hille, B. *Ionic Channels of Excitable Membranes*, 2nd ed. Sinauer Associates, Sunderland, MA, 341 (1992).
11. Frace, A. M., and H. C. Hartzell. Opposite effects of phosphatase inhibitors on L-type calcium and delayed rectifier currents in frog cardiac myocytes. *J. Physiol. (Lond.)* **472:**305–326 (1993).
12. Tamaoki, T., H. Nomoto, I. Takahashi, Y. Kato, M. Morimoto, and F. Tomita. Staurosporine, a potent inhibitor or phospholipid/Ca dependent protein kinase. *Biochem. Biophys. Res. Commun.* **135:**397–402 (1986).
13. Rhegg, U. T., and G. M. Burgess. Staurosporin, K-252, and UCN-01: potent but nonspecific inhibitors of protein kinases. *Trends Pharmacol Sci.* **10:** 18–22 (1989).
14. Lacerda, A. E., D. Rampe, and A. M. Brown. Effects of protein kinase C activators on cardiac Ca^{2+} channels. *Nature (Lond.)* **335:**249–251 (1988).
15. Eicholtz, T., D. B. deBont, J. deWidt, R.-M. Liskamp, and H.-L. Ploegh. A myristoylated pseudosubstrate peptide, a novel protein kinase C inhibitor. *J. Biol. Chem.* **268:**1982–1986 (1993).
16. Bahinski, A., A. C. Nairn, P. Greengard, and D. C. Gadsby. Chloride conductance regulated by cyclic AMP-dependent protein kinase in cardiac myocytes. *Nature (Lond.)* **340:**718–721 (1989).
17. Harvey, R. D., and J. R. Hume. Autonomic regulation of a chloride current in heart. *Science (Washington D. C.)* **244:**983–985 (1989).
18. Ehara, T., and K. Ishihara. Anion channels activated by adrenaline in cardiac myocytes. *Nature (Lond.)* **347:**284–286 (1990).
19. Hagiwara, N., H. Matsuda, M. Shoda, and H. Irisawa. Stretch-activated anion currents of rabbit cardiac myocytes. *J. Physiol. (Lond.)* **456:**285–302 (1992).
20. Sorota, S. Swelling-induced chloride-sensitive current in canine atrial cells revealed by whole-cell patch-clamp method. *Circ. Res.* **70:**679–687 (1992).
21. Sipido, K., G. Callewaert, and E. Carmeliet. $[Ca^{2+}]_i$ transients and $[Ca^{2+}]_i$-dependent chloride current in single Purkinje cells from rabbit heart. *J. Physiol. (Lond.)* **468:**641–667 (1993).
22. Kawano, S., Y. Hirayama, and M. Hiraoka. Activation mechanism of Ca^{2+}-sensitive transient outward current in rabbit ventricular myocytes. *J. Physiol. (Lond.)* **486:**593–604 (1995).
23. Walsh, K. B., and K. J. Long. Properties of a protein kinase C-activated chloride current in guinea pig ventricular myocytes. *Circ. Res.* **74:**121–129 (1994).
24. Zhang, K., P. L. Barrington, R. L. Martin, and R. E. Ten Eick. Protein kinase-dependent Cl^- currents in feline ventricular myocytes. *Circ. Res.* **75:**133–143 (1994).
25. Collier, M. L., and J. R. Hume. Unitary chloride channels activated by protein kinase C in guinea pig ventricular myocytes. *Circ. Res.* **76:**317–324 (1995).
26. Faux, M. C., and J. D. Scott. Molecular glue: kinase anchoring and scaffold proteins. *Cell* **85:**9–12 (1996).
27. Klauck, T. M., M. C. Faux, K. Labudda, L. K. Langeberg, S. Jaken, and J. D. Scott. Coordination of three signalling enzymes by AKAP79, a mammalian scaffold protein. *Science (Washington D. C.)* **271:**1589–1592 (1996).
28. Johnson, B. D., T. Scheuer, and W. A. Catterall. Voltage-dependent potentiation of L-type Ca^{2+} channels in skeletal muscle cells requires anchored cAMP-dependent protein kinase. *Proc. Natl. Acad. Sci. USA* **91:**11492–11496 (1994).
29. Gray, P. C., V. C. Tibbs, W. A. Catterall, and B. J. Murphy. Identification of a 15-kD cAMP-dependent protein kinase-anchoring protein associated with skeletal muscle L-type calcium channels. *J. Biol. Chem.* **272:**6297–6302 (1997).
30. Ono, K., and H. A. Fozzard. Phosphorylation restores activity of L-type calcium channels after rundown in inside-out patches from rabbit cardiac cells. *J. Physiol. (Lond.)* **454:**673–688 (1992).
31. Hescheler, J., M. Kameyama, W. Trautwein, G. Mieskes, and H. D. Söling. Regulation of the cardiac calcium channel by protein phosphatases. *Eur. J. Biochem.* **165:**261–266 (1987).
32. Hescheler, J., G. Mieskes, J. C. Rhegg, A. Takai, and W. Trautwein. Effects of a protein phosphatase inhibitor, okadaic acid, on membrane currents of isolated guinea-pig cardiac myocytes. *Pflueg. Arch. Eur. J. Physiol.* **412:** 248–252, 1988.
33. Cheng, S. H., D. P. Rich, J. Marshall, R. J. Gregory, M. J. Welsh, and A. E. Smith. Phosphorylation of the R domain by cAMP-dependent protein kinase regulates the CFTR chloride channel. *Cell* **66:**1027–1036 (1991).
34. Nakashima, Y., and K. Ono. Rate-limiting steps in activation of cardiac Cl^- current revealed by photolytic application of cAMP. *Am. J. Physiol.* **267:**H1514–H1522 (1994).

Send reprint requests to: Dr. H. Criss Hartzell, Department of Cell Biology, Emory University School of Medicine, 1648 Pierce Drive, Atlanta, GA 30322-3030. E-mail: criss@anatomy.emory.edu